Supercontinuum generation from ~1.9 to 4.5 μm in ZBLAN fiber with high average power generation beyond 3.8 μm using a thulium-doped fiber amplifier

Ojas P. Kulkarni,[1,*] Vinay V. Alexander,[1] Malay Kumar,[1] Michael J. Freeman,[2,†] Mohammed N. Islam,[1,2,§] Fred L. Terry, Jr.,[1] Manickam Neelakandan,[3] and Allan Chan[3]

[1]*University of Michigan, Ann Arbor, Michigan 48109, USA*
[2]*Omni Sciences Inc., Ann Arbor, Michigan 48105, USA*
[3]*U.S. Army Communications–Electronics Research, Development and Engineering Center, Intelligence and Information Warfare Directorate (CERDEC I2WD), Aberdeen Proving Ground, Maryland 21005, USA*
**Corresponding author: ojaspk@umich.edu*

Received June 7, 2011; accepted August 1, 2011;
posted August 31, 2011 (Doc. ID 148897); published September 26, 2011

A mid-IR supercontinuum (SC) fiber laser based on a thulium-doped fiber amplifier (TDFA) is demonstrated. A continuous spectrum extending from ~1.9 to 4.5 μm is generated with ~0.7 W time-average power in wavelengths beyond 3.8 μm. The laser outputs a total average power of up to ~2.6 W from ~8.5 m length of ZrF_4—BaF_2—LaF_3—AlF_3—NaF (ZBLAN) fiber, with an optical conversion efficiency of ~9% from the TDFA pump to the mid-IR SC. Optimal efficiency in generating wavelengths beyond 3.8 μm is achieved by reducing the losses in the TDFA stage and optimizing the ZBLAN fiber length. We demonstrate a novel (to our knowledge) approach of generating modulation instability-initiated SC starting from 1.55 μm by splitting the spectral shifting process into two steps. In the first step, amplified approximately nanosecond-long 1.55 μm laser diode pulses with ~2.5 kW peak power generate a SC extending beyond 2.1 μm in ~25 m length of standard single-mode fiber (SMF). The ~2 μm wavelength components at the standard SMF output are amplified in a TDFA and coupled into ZBLAN fiber leading to mid-IR SC generation. Up to ~270 nm SC long wavelength edge extension and ~2.5× higher optical conversion efficiency to wavelengths beyond 3.8 μm are achieved by switching an Er:Yb-based power amplifier stage with a TDFA. The laser also demonstrates scalability in the average output power with respect to the pulse repetition rate and the amplifier pump power. Numerical simulations are performed by solving the generalized nonlinear Schrödinger equation, which show the long wavelength edge of the SC to be limited by the loss in ZBLAN.

OCIS codes: 190.4370, 320.6629.

1. INTRODUCTION

We have demonstrated, for the first time to our knowledge, a mid-IR supercontinuum laser (MISCL) using a thulium-doped power amplifier stage. The MISCL provides a continuous spectrum extending from ~1.9 to 4.5 μm with ~0.7 W time-average power in wavelengths beyond 3.8 μm. SC output of ~2.6 W is generated with ~9% conversion efficiency from the thulium-doped fiber amplifier (TDFA) pump to the MISCL output. Higher efficiency mid-IR SC generation is achieved by implementing a large mode area (LMA) Tm-based power-amp stage and shifting the SC pump wavelength from 1.55 to ~2 μm.

Mid-IR SC generation starting from 1.55 μm laser diode pulses using modulation instability (MI)-initiated pulse breakup has been demonstrated in the past [1]. Such a technique is beneficial, since it leverages the maturity of fiber-coupled telecommunication wavelength components to generate a high time-average power SC extending into the mid-IR. Previously demonstrated MISCL systems use all Er:Yb-based high power amplification stages. We demonstrate a novel method whereby the Er:Yb power-amp stage is replaced by, first, a 1.55 to ~2 μm wavelength-shifting stage, followed by a Tm-doped power-amplifier stage. The TDFA-based MISCL generates wavelengths beyond 3.8 μm with ~2.35% efficiency with respect to the power-amp pump, which is ~2.5 times more efficient than an Er:Yb power-amp-based system. The long wavelength edge of the generated continuum in the Tm-based system also extends ~270 nm further. The demonstrated TDFA-based system also retains the advantages of being all-fiber-integrated, having no moving parts, and exhibits power scalability with pulse repetition rate and amplifier pump power, as previously demonstrated by a MISCL with all 1.55 μm amplification stages [1].

The TDFA-based system generates a mid-IR SC in two steps. In the first step, a fused silica continuum extending to beyond 2.1 μm is generated by launching amplified, nanosecond-long 1.55 μm laser diode pulses into an ~25 m length of standard single-mode fiber (SMF). A thulium-based power-amp stage amplifies ~2 μm light components in the output of the standard SMF continuum. By coupling the power-amp output to a ~8.5 m length of ZBLAN fiber, spectral extension into the mid-IR is observed. Higher, longer wavelength generation efficiency is achieved by reducing TDFA system losses and through optimization of the ZBLAN fiber length and the first step SC generation parameters in the standard SMF. Numerical simulations are also performed by solving

the generalized nonlinear Schrödinger equation (GNLSE) to compare and extend experimental results.

2. MOTIVATION AND BACKGROUND

Light generation in the mid-IR wavelength range from 2 to 5 μm is beneficial for a number of applications, including spectroscopy [2], explosive and chemical detection [3,4], remote sensing and ranging [5], free-space communications [6], and medicine [7]. Currently available solid-state laser technologies operating in the mid-IR wavelength range include quantum cascade lasers (QCLs) [8], optical parametric oscillators (OPOs) [9,10], and rare-earth-doped ZBLAN fiber lasers [11]. In comparison, SC sources are attractive because they can cover several octaves of light, thus increasing the sensitivity and selectivity of spectroscopic studies [12].

One technique to reliably generate a mid-IR SC is by shifting light from a near-IR laser into the mid-IR wavelengths using nonlinear optical processes. In ZBLAN fibers, an SC extending to ~6.28 μm has been demonstrated by pumping an ~2 cm length of fiber with mode-locked 1480 nm pulses of ~50 MW peak power and 20 mW average power [13]. Another mid-IR SC fiber laser demonstration based on ZBLAN fiber used a 1550 nm mode-locked Er-doped laser and generated ~5 mW in the wavelength range from 1.8 to 3.4 μm [2]. Fibers based in high nonlinearity materials such as tellurite have also been used for SC generation. For example, continuum extending from ~0.8 to 4.87 μm with 90 mW output average power has been demonstrated by coupling 110 fs long, 1.55 μm pulses into a 0.8 cm length of tellurite photonic crystal fiber (PCF) [14].

A novel technique to eliminate the need of mode-locked lasers for high peak power pulse generation has been previously demonstrated. In this technique, modulation instability in standard SMF is used to initiate pulse breakup of quasi-CW laser diode pulses [15]. Typically, 1 ns long 1.55 μm laser diode pulses are first amplified through two or more stages of Er/Er:Yb fiber amplifiers. After initiating pulse breakup in a few meter lengths of standard SMF, an SC extending from 0.8 to 4.4 μm has been generated in ~7 m length of ZBLAN fiber, with 23 mW average power output [16]. Also, using linear scaling of the time-average power with the pulse repetition rate, up to 10.5 W average power output in a continuum extending from 0.9 to 3.8 μm has been demonstrated [1]. More recently, by using ~20 kW 1.55 μm peak power pulses and longer lengths of ZBLAN fibers (~12 m), a high average power spectrum extending out to ~4.2 μm has been achieved using all 1.55 μm amplification stages [17].

In this paper, we demonstrate an all-fiber integrated mid-IR SC laser, based on a Tm-doped power-amplifier stage. The motivation to incorporate a TDFA stage is driven by the higher pump-to-signal conversion efficiency demonstrated in Tm-doped gain fibers compared to Er:Yb fiber amplifiers (EYFAs). For example, slope efficiency as high as 56% is demonstrated in LMA Tm-doped gain fiber [18] compared to LMA-EYFAs, which have demonstrated slope efficiencies of ~38% [19] in comparable fiber geometries. Also, shifting the SC pump from 1.55 to ~2 μm is pursued with an attempt to generate a longer extending SC in the mid-IR wavelengths.

Various techniques to generate ~2 μm light pulses for input to TDFAs have been demonstrated. For example, by using a mode-locked Er fiber laser with polarization-maintaining components operating at 1557 nm followed by an EYFA, a Raman shifting soliton pulse to ~2 μm in a 12 m length of high NA fiber has been demonstrated in the past [20]. A subsequent dispersion-managed LMA-TDFA stage generates pulses with up to 230 kW peak power at ~2 μm. Another approach generates ~750 fs long ~1.95 μm pulses using a saturable absorber based on carbon nanotubes in a Tm-doped fiber laser cavity [21]. Techniques using ~1.55 μm laser diode pulses instead of mode-locked lasers have also been demonstrated. One approach involves successive orders of cascaded Raman wavelength shifting in germanium-doped fused silica fibers with a NA of ~0.41 [22]. In this approach, up to three orders of shifting from 1.53 μm leads to light generation at 1.94 μm. Another demonstrated technique involves gain switching a Tm-doped fiber cavity with a modulated 1.55 μm pump to generate 10 ns long 2 μm pulses [23].

In our approach, ~1 ns long laser diode pulses at 1.55 μm are amplified to ~2.5 kW peak power. Pulse breakup through modulation instability and long wavelength shifting through Raman processes in an ~25 m length of standard SMF give rise to ~2 μm pulsed light components for input to a Tm-doped fiber amplifier. The technique eliminates the need for mode-locked lasers for high peak power pulse generation at ~2 μm and uses all standard telecommunication wavelength fiber-coupled components. Also, due to the absence of a regenerative cavity, the system does not require any bulk 2 μm optical isolators to prevent feedback from spontaneous emission or spurious reflection from subsequent TDFA or SC generating stages.

The paper is organized as follows. We describe the TDFA-based mid-IR SC laser setup in Section 3. In Section 4, we present the experimental results of SC generation, efficiency characterization, and optimization. Simulation modeling and results are presented in Section 5. In Section 6, we discuss the experimental and simulation results, and finally we summarize our findings in Section 7.

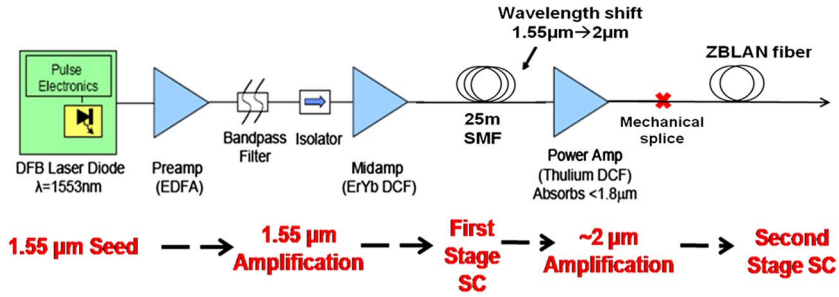

Fig. 1. (Color online) Schematic of experimental setup depicting two-stage mid-IR SC generation using TDFA. DCF, dual-cladding fiber.

3. EXPERIMENTAL SETUP

The block diagram of the experimental setup is shown in Fig. 1. The seed laser consists of a 1553 nm distributed feedback (DFB) laser diode with ~1 ns long pulses output at a repetition rate adjustable from a few MHz down to ~10 kHz. The laser diode pulses are amplified through two stages—a single-mode Er-doped fiber amplifier (EDFA; preamp) followed by a cladding-pumped Er:Yb-doped midamp. The preamp stage consists of an ~2 m length of 4/125 μm gain fiber pumped by up to 400 mW at 980 nm. A 100 GHz line width optical add–drop multiplexer at the signal wavelength is used to filter out amplified spontaneous emission (ASE) generated in the preamp stage. The midamp stage consists of ~5 m of cladding-pumped 7/130 μm Er:Yb codoped fiber pumped by a single 10 W, 976 nm laser diode.

A near-IR continuum starting from 1.55 μm is first generated in standard SMF. The midamp is used to boost the peak power level of the optical pulses to the few kilowatt level, and the output is spliced to an ~25 m length of standard SMF. For the case of the midamp output, the peak power of the pulses can be estimated from their duty cycle and the measured average power at the output of the amplifier. For example, with a pulse width of ~1 ns and a pulse repetition rate of 500 kHz, 1 W output from the midamp corresponds to ~2 kW peak power of the individual pulses.

The output of the standard SMF-based 2 μm light source is spliced to an LMA-TDFA, which serves as the power amp. LMA gain fiber is chosen to reduce nonlinear effects in the amplifier and has core/cladding dimensions of 25/250 μm. The gain fiber has a low core NA of ~0.1 to reduce the multimodedness in the fiber at 2 μm wavelength, which is achieved in Tm-doped fibers by a raised refractive index pedestal layer surrounding the fiber core [18]. The gain fiber has a rated peak absorption of 5 dB/m at 793 nm, and a 4.5 m length is chosen to provide sufficient pump depletion. The mode conversion from standard SMF to LMA gain fiber is achieved by a pump combiner/mode adapter with a 10/125 μm fiber at the input and a 25/250 μm passive fiber matched geometrically to the Tm gain fiber at the output. The output of the Tm gain fiber is spliced to a second pump combiner/mode adapter, which has a dual-clad output fiber with 10/125 μm core/cladding diameters, allowing for convenient coupling to the ZBLAN fiber. In addition, the output combiner combines two fiber-coupled 35 W, 790 nm pump lasers with 105 μm core diameter, 0.22 NA fiber pigtails in to the gain fiber to form a backward-pumped amplifier configuration. The gain fiber is heat sunk by coiling it around a copper mandrel with grooves matched to fit the gain fiber.

In another implementation of the TDFA, a small-core gain fiber with core/cladding dimensions of 10/130 μm is used. The small-core setup provides direct splicing of the standard SMF output to the TDFA input. A single combiner on the output side couples pump light into the gain fiber in the backward-propagating direction.

The 35 W pump diodes used in the setup demonstrate a FWHM of ~1.2 nm with center wavelengths of ~791 nm and typical threshold currents of 8 A. The electro-optical efficiency of the lasers is specified to be ~41% with 35 W output at ~49 A current. The pump is mounted on a thermoelectric (TE) cold plate to temperature tune the pump wavelength. A thermistor mounted on the cold plate provides feedback to the electronic circuit driving the current in the cold plate to keep the diode temperature stable during operation. The current through the two pump lasers is modulated by a square wave with 50% duty cycle at ~250 Hz to reduce the thermal load in the system and allow for modulation of the SC output without a need for external chopping equipment. The modulation is achieved by connecting the two pumps in series with a MOSFET switch driven by a signal generator. A bank of resistors is also included in the circuit to provide current limiting along with other safety measures to prevent damage to the pumps due to parasitic currents. For driving the pump diodes with CW current, the signal generator is replaced by a 9 V battery to keep the MOSFET switch turned on.

The ZBLAN fiber used in the experiments has a high NA of ~0.27 to reduce bend-induced losses at wavelengths beyond 4 μm. The fiber has a cutoff wavelength of ~2.75 μm and a core/cladding diameter of 8/125 μm as specified by the manufacturer. The fiber zero-dispersion wavelength (ZDW) is expected to be ~1.65 μm based on the material dispersion parameter of ZBLAN [24].

The output from the TDFA is mechanically spliced to the ZBLAN input with angle-cleaves on either fiber to prevent reflections in the system. Careful matching of the fiber angles is achieved by observation through a microscope for optimum coupling. The observed mechanical splice loss ranges from 45% to 50%, depending on the quality of the splices and the proximity of the fibers. The output from the ZBLAN fiber is measured with a thermal power meter, and power distribution in various spectral bands is measured using suitable cut-off long-pass filters. The spectrum is measured by a Czerny—Turner monochromator and a TE-cooled HgCdTe detector.

4. EXPERIMENTAL RESULTS

A. LMA-TDFA-Based Mid-IR SC Laser Spectrum

The output spectrum of an ~8.5 m length of ZBLAN fiber mechanically spliced to the LMA-TDFA is shown in Fig. 2. The spectrum extends from ~1.9 to 4.5 μm with ~2.6 W total average power, of which ~0.7 W lies in wavelengths beyond 3.8 μm. The TDFA is pumped with ~30 W of 790 nm pump power with 50% modulation and outputs ~8 W of average power around 2 μm. The input to the TDFA comprises output from an ~25 m length of standard SMF with ~2.5 kW peak power 1.55 μm laser diode input pulses of ~1 ns duration at 500 kHz repetition rate. The mechanical splice loss is observed to be ~45%, corresponding to a coupled pump power of ~4.4 W. The residual power in the 1.8–2.1 μm wavelengths at the output of the ZBLAN fiber is ~0.13 W and is calculated

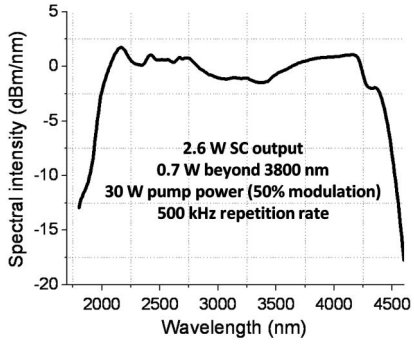

Fig. 2. Mid-IR SC spectrum from ~8.5 m ZBLAN fiber pumped with TDFA extending from ~1.9 to 4.5 μm.

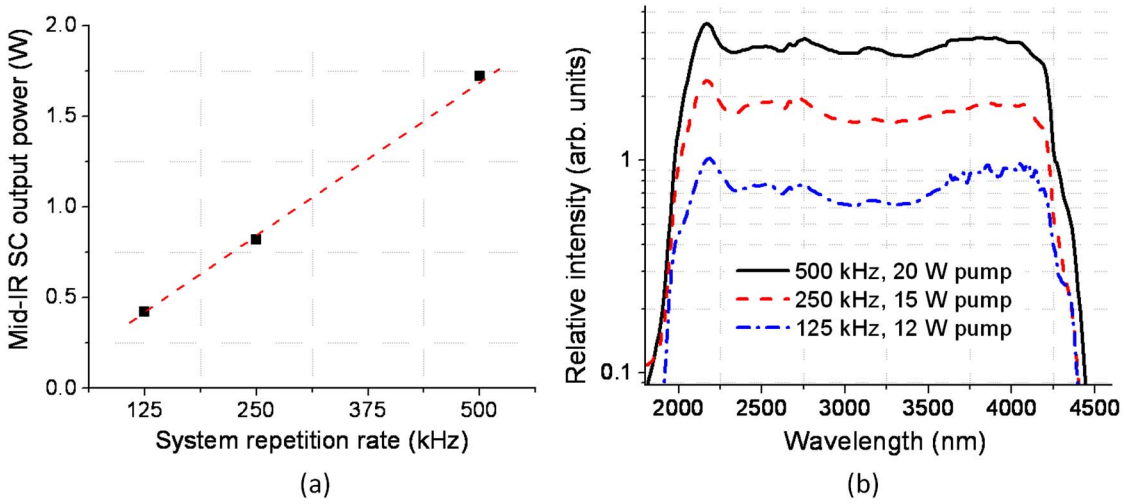

Fig. 3. (Color online) Output from 8.5 m length of ZBLAN showing power scaling with repetition rate and 790 nm pump power: (a) output time-average power, (b) output spectrum.

from the area under the curve in the calibrated spectrum in these wavelengths, indicating ~97% SC pump depletion. With the modulation of the TDFA pumps with a 50% duty cycle square wave at 250 Hz, the SC output is also modulated. Hence an observed SC output power of 2.6 W corresponds to ~5.2 W SC output during the ON phase of the 250 Hz modulation signal. Similarly, the ~0.7 W average power measured in wavelengths beyond 3.8 μm indicates ~1.4 W power output from the laser in these wavelengths for 50% of the time.

The generated SC is continuous, with a spectral power density >0 dBm/nm (1 mW/nm) between ~3.6 and 4.3 μm. The intensity of the measured spectrum is calibrated in dBm/nm as follows. First, the measured SC spectrum is corrected for the spectral responsivity of the HgCdTe detector and the monochromator grating response. The spectral power density is then calculated using the SC output power in the 3.5–3.8 μm wavelength region measured by the thermal power meter and appropriate wavelength filters. The SC laser generates ~0.9 W beyond 3.5 μm. The dip in the spectrum at ~4.25 μm is attributed to the CO_2 absorption in the atmosphere while traversing the ~0.75 m path length inside the monochromator [25].

Figure 3 shows the power scaling of the TDFA-based mid-IR SC laser as a function of the pulse repetition rate and the 790 nm pump power. By varying the pulse repetition rate electronically, the demonstrated Tm system shows versatility in its ability to adjust the output power with similar spectral extent. Figure 3(a) shows the linear scaling of the average power at the output of an 8.5 m length of ZBLAN fiber over 125–500 kHz pulse repetition rates, while Fig. 3(b) shows the corresponding output spectrum. The spectrum out of the ZBLAN fiber has similar spectral extent and shape; however, the average power content scales linearly with the pulse repetition rate. The preservation of the spectral shape with increasing repetition rate shows that the doubling of the output average power with doubling of the pulse repetition rate is achieved by increasing the frequency of occurrence of the pulses while maintaining similar pulse peak powers. Figure 3 also shows that the amount of 790 nm pump power required to double the output average power with pulse repetition rate does not scale linearly. For example, at 125 kHz, the SC laser outputs ~0.4 W average power at 12 W of modulated pump power. However, to double the output average power to ~0.8 W at 250 kHz, only ~3 W of additional modulated pump power is required, suggesting ~13% slope efficiency with system repetition rate. The increase in efficiency with repetition rate is attributed to the threshold of the TDFA (~6 W) and the increase in amplifier efficiency at higher pulse duty cycles due to lower losses to spontaneous emission.

Figure 4 compares the SC spectrum generated by ~8.5 m ZBLAN fiber pumped by a TDFA power amp to the best EYFA power-amp results observed to date from an ~12 m length of ZBLAN fiber with identical properties [17]. The observed long wavelength SC edge from the TDFA-based mid-IR source extends ~270 nm beyond the EYFA system output. The extension in the long wavelength edge is attributed to shifting of the SC pump from 1.55 to ~2 μm in the TDFA system. Figure 4 also shows that the EYFA-SC extends in either direction around the ~1.55 μm SC pump. In comparison, the TDFA-SC extends only toward the longer wavelengths with respect to the SC pump at ~2 μm. The difference in the nature of the spectral broadening between the two systems is attributed to the dispersion properties of ZBLAN material, which has a ZDW around 1.65 μm [24]. As a result, pumping the ZBLAN fiber at ~2 μm compared to 1.55 μm amounts to shifting the SC pump into the anomalous dispersion regime, where spectral broadening is observed to occur largely through stimulated Raman processes without much contribution from self-phase modulation (SPM) as observed in EYFA systems.

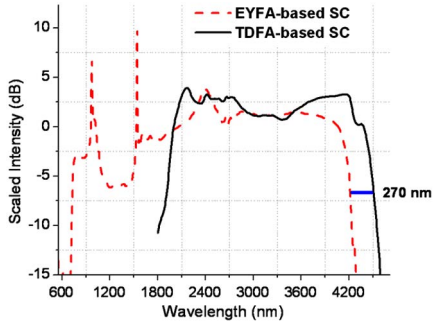

Fig. 4. (Color online) Mid-IR SC spectrum from 8.5 m ZBLAN in TDFA power amp system compared to 12 m ZBLAN in EYFA-based system [17].

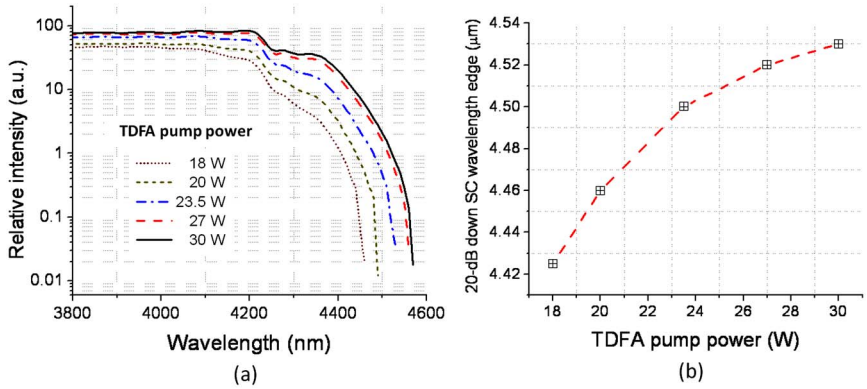

Fig. 5. (Color online) Evolution of the long wavelength SC edge in 8.5 m ZBLAN fiber length as a function of TDFA pump power measured at 500 kHz pulse repetition rate: (a) spectrum, (b) long wavelength edge.

The evolution of the long wavelength edge of the 8.5 m ZBLAN fiber output as a function of modulated TDFA pump power at 500 kHz pulse repetition rate is shown in Fig. 5(a). At a fixed repetition rate, higher TDFA pump power corresponds to higher peak output powers and, hence, a longer extending SC spectrum. Figure 5(b) plots the −20 dB SC wavelength edge of the measured spectra versus the modulated TDFA pump powers with saturation in the wavelength edge beyond ~4.5 μm. The long wavelength edge of the SC is limited by the absorption edge of the ZBLAN fiber. For example, at 4.5 μm, the absorption loss in the fiber is expected to be ~1 dB/m, suggesting that any generated components at longer wavelengths in the ~8.5 m length of ZBLAN undergo rapid attenuation, preventing further spectral extension.

B. LMA-TDFA-Based SC Laser Efficiency

The thermal power meter measurements for the TDFA output, 8.5 m ZBLAN SC output, and spectral content beyond 3.8 μm at the output of the ZBLAN fiber are plotted against the corresponding modulated TDFA pump power in Fig. 6. The LMA-TDFA operated in backward-pumped configuration shows an overall efficiency of ~27% with ~8 W output power at ~30 W of 790 nm pump power. Observed SC output power of ~2.6 W corresponds to an overall mid-IR output efficiency of ~9% with respect to the 790 nm pump. ~0.7 W of the ZBLAN output lies in wavelengths beyond 3.8 μm, leading to an observed efficiency of ~2.35% in generating wavelengths >3.8 μm with respect to the TDFA pump power.

Table 1 summarizes the efficiency of various components of the TDFA-based MISCL. The Er:Yb midstage amplifier in the setup outputs ~1.25 W of average power around 1.55 μm. The first SC section, comprising ~25 m standard SMF spliced

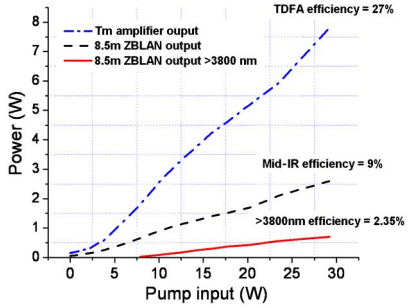

Fig. 6. (Color online) Power meter measurement of TDFA output, 8.5 m ZBLAN SC output, and output average power beyond 3.8 μm versus TDFA pump power.

to the midamp, outputs ~1 W total power, of which ~0.59 W lies in wavelengths beyond 1.8 μm, where TDFA gain occurs. The efficiency of the TDFA stage is maximized by optimizing the splices between the LMA gain fiber and the pump combiner fibers and heat sinking the Tm gain fiber. Also, active cooling of the 35 W pump diodes allows pumping of the amplifier close to 793 nm, where the maximum rated pump absorption in the gain fiber occurs. The length of the fiber between the TDFA output combiner and the ZBLAN fiber is kept at a minimum practically permissible length of ~0.5 m to reduce nonlinear losses in its ~10 μm diameter core. Approximately 55% coupling efficiency is observed at the mechanical splice from the TDFA output to the ZBLAN fiber due to the mode mismatch between the ~10 μm core diameter combiner output fiber and the high NA ZBLAN fiber with an ~8 μm core diameter.

The length of ZBLAN fiber used in the mid-IR SC generation is optimized for efficient generation of wavelengths beyond 3.8 μm. Three different lengths of ZBLAN fiber (5.5, 8.5, and 13 m) were used in the setup. The power generated in wavelengths beyond 3.8 μm was measured as a function of the TDFA average output power at a fixed repetition rate of 500 kHz, and the observed results are plotted in Fig. 7. It is observed that for the ~13 m length of ZBLAN fiber, the long wavelength power generation saturates at higher TDFA output powers compared to the result from the ~8.5 m length. On the other hand, the ~5.5 m length does not generate as much long wavelength power for the same amount of TDFA output power, indicating lower long wavelength efficiency. Based on the result, we observe ~8.5 m length to be optimal for higher efficiency long wavelength generation. For longer lengths of ZBLAN, the longer wavelength components undergo additional attenuation in the excess length of ZBLAN fiber. In comparison, the 5.5 m length is found to be short of optimal length and would require higher peak power output from the TDFA to generate power in longer wavelengths more efficiently.

C. First Stage Optimization

The output from an ~25 m length of standard SMF for various peak power settings of the 1.55 μm input pulse is shown in Fig. 8(a). Light generation in the TDFA gain band extending from ~1.75 to 2.1 μm [26] is observed at input powers as low as ~1 kW, with a longer extending spectrum at higher peak powers. At ~2.5 kW peak power, a flat continuum extending from ~1.5 to 2.25 μm, covering the entire TDFA gain band, is

Table 1. Efficiency of Various Components of the TDFA-pumped ZBLAN Mid-IR SC Laser[ab]

System Component	Definition	Efficiency
790 nm pump diode	Electro-optic efficiency provided by manufacturer	~41%
Er:Yb midamp	1.55 μm output/976 nm CW pump power	~17%
25 M SMF	Output > 1.8 μm/input power	~47%
LMA-TDFA	~2 μm output/790 nm modulated pump power	~27%
Mechanical splice	Coupled ~2 μm/tdfa-output	~55%
>3.8 μm light-shifting efficiency	Power beyond 3.8 μm/coupled ~ 2 μm power	~16%
SC generation efficiency	SC output/coupled ~ 2 μm power	~59%

[a]TDFA pump to SC conversion efficiency = $0.27 \times 0.55 \times 0.59 = 9\%$.
[b]TDFA pump to >3.8 μm conversion efficiency = $0.27 \times 0.55 \times 0.16 = 2.35\%$.

obtained from an ~25 m length of standard SMF. Figure 8(b) shows the effect of the first stage input peak power on the spectrum output of an ~12 m length of ZBLAN fiber for a fixed CW TDFA pump power of ~8 W. At low TDFA pump powers, the spectral extent of the ZBLAN output is found to be heavily dependent on the peak power used for 2 μm light generation. For example, the 1.5 kW peak power case used for 2 μm light generation yields the longer extending ZBLAN output spectra compared to the 2.5 kW case. However, the ASE peak from the TDFA in the ZBLAN output is ~8 times higher in the 1.5 kW case compared to 2.5 kW due to insufficient strength of the input signal in the TDFA gain band. Hence, even though the SC extends to beyond 4 μm at lower first stage peak powers, the efficiency of SC generation is poor in the 1–1.5 kW peak power cases.

Figure 8(c) shows the relative power in wavelengths >2.5 μm plotted against the peak power used at the input of the standard SMF. The result shows that higher spectral shifting efficiency is achieved at 2.5 kW peak power compared to lower peak powers, with saturation observed beyond 2 kW. Above 2.5 kW, the standard SMF generates additional components beyond 2.1 μm, which are not efficiently amplified in the TDFA. By pumping the TDFA with higher pump power, a spectrum extending to 4.5 μm with ~97% pump depletion is obtained, as shown in Fig. 2, for first stage peak powers of ~2.5 kW to provide higher efficiency long wavelength generation. However, the demonstrated result shows the flexibility in extent of spectral generation in the two-step SC scheme based on the availability of pump power in the system and the application requirement.

Figure 9 shows the effect of the length of standard SMF used in the first stage on the output spectrum from the ZBLAN fiber. Three lengths of standard SMF are used (10, 25, and 50 m), and in each case, the 1.55 μm peak power is adjusted so that the same average power (~0.6 W) is generated beyond 1.8 μm at the output of the fiber, measured using a power meter placed after a Ge long-pass filter. The standard SMF output is spliced to the LMA-TDFA, and the output spectrum from the ~8.5 m length of ZBLAN at ~20 W of pump power is measured in each case. Figure 9 shows that the SMF length used in the 2 μm light generation does not influence the extent of ZBLAN output as long as similar average powers are

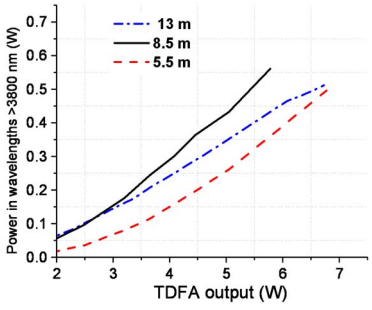

Fig. 7. (Color online) Experimental optimization of power generation beyond 3.8 μm for various lengths of ZBLAN fibers.

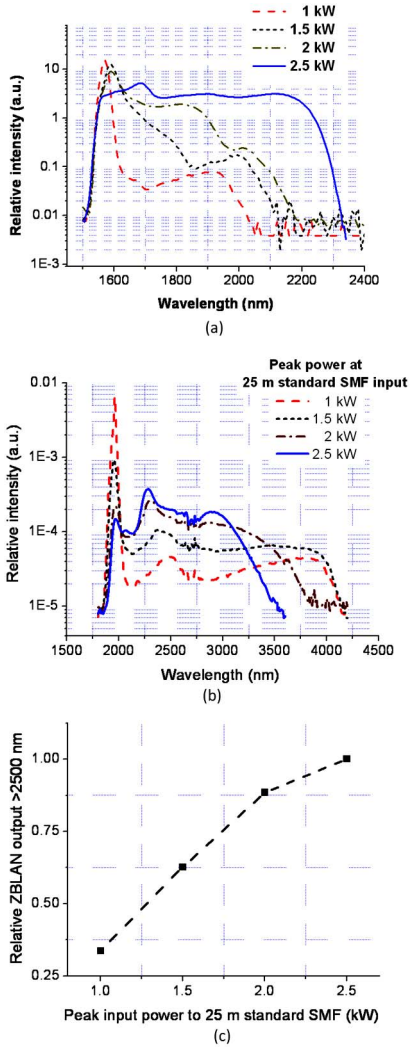

Fig. 8. (Color online) Stage 1 peak power optimization: (a) output spectrum from ~25 m standard SMF for various peak input powers of 1.55 μm pulses, (b) 12 m ZBLAN output at ~8 W CW TDFA pump power for various 1.55 μm peak powers used in 2 μm light generation, (c) relative average power generated beyond 2.5 μm at output of ~12 m ZBLAN as a function of the stage 1 peak power for fixed TDFA pump power.

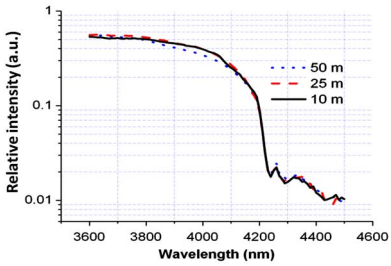

Fig. 9. (Color online) ~8.5 m ZBLAN output at ~20 W TDFA pump power for various standard SMF lengths in the first stage.

generated in the TDFA gain band at the output of the standard SMF. The observed result can be explained by the fact that since the standard SMF with ZDW ~1.3 μm is pumped at 1.55 μm in the anomalous dispersion regime, soliton propagation is supported in the fiber from the balance of pulse broadening and compression through dispersion and fiber nonlinearities. Therefore, the soliton pulses at the output of 50 m length of standard SMF do not undergo much broadening compared to higher peak power pulses used in the generation of similar spectra from only 10 m length. Also, the dispersion length of the fiber is several kilometers for nanosecond-long pulses in standard SMF, and hence dispersive effects are not expected to be dominant. Therefore, the choice of SMF length can be made on the basis of ease of peak power generation from the Er:Yb midamp, with shorter fiber lengths requiring higher peak power pulses. Also, the low cost of standard SMF does not provide any incentive to use shorter fiber lengths, and 25 m standard SMF length is chosen as optimal. The results indicate that in applications where remote delivery of the 2 μm light is required, the length of standard SMF can be chosen depending on the setup requirements without appreciable degradation in the performance of the mid-IR SC laser, providing additional flexibility for practical applications.

D. Small-Core TDFA-Based Mid-IR SC Spectrum

The mid-IR SC spectrum from the small-core TDFA-based setup is shown in Fig. 10. The small-core TDFA (10/130 μm core/cladding diameter) is pumped with a maximum CW pump power of ~8 W with optimal settings in the first stage and a pulse repetition rate of 50 kHz. The TDFA output is mechanically spliced to an ~12 m length of ZBLAN fiber. A spectrum extending from ~1.9 to 4.3 μm is obtained with ~300 mW average output power, of which ~85 mW lies in wavelengths beyond 3.8 μm. The peak in the observed spectrum at ~2 μm corresponds to the ASE generated in the amplifier and any undepleted SC pump. The wiggles in the spectrum around

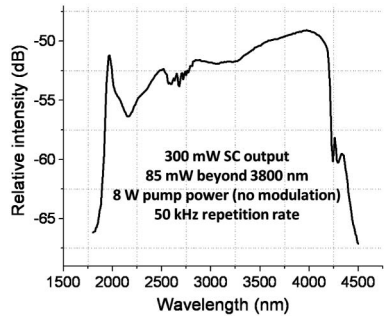

Fig. 10. Output spectrum from ~12 m length of ZBLAN fiber with spectrum extending from 1.9 to 4.5 μm.

2.7 μm correspond to water vapor absorption, and those at ~4.25 μm are due to CO_2 absorption in the air during propagation in the monochromator.

Compared to the LMA system, the small-core TDFA system shows less overall efficiency. For example, the efficiency in the generation of wavelengths beyond 3.8 μm with respect to the TDFA pump power is ~1.1% in the small-core system, compared to ~2.35% observed in the LMA system. One of the main factors contributing to the lower efficiency of the small-core system is the higher nonlinearity in the amplifier. In the case of the above result, we observe ~15% pump-to-signal conversion efficiency in the small-core amplifier with respect to the coupled pump power. The higher nonlinearity in the small-core gain fiber leads to shifting of ~2 μm amplified pulses to longer wavelengths within the amplifier, which reduces the length of the gain fiber for which the input signal lies spectrally in the amplifier gain band. Lower nonlinearity in the amplifier is also preferred to achieve efficient coupling to the ZBLAN fiber. For example, at 2.4 μm wavelength, the mode field diameter in the 10 μm core amplifier fiber is expected to increase to ~14 μm, which increases the free-space coupling loss to the 8 μm core ZBLAN fiber due to larger mode-area mismatch. The small-core TDFA system is also observed to be limited in its average power scaling capability, with damage consistently observed at the combiner fiber and gain fiber splice at CW pump powers >26 W at 400 kHz pulse repetition rate. The setup however, can be used for low power applications with passively cooled 790 nm pump lasers and a single small-core combiner for coupling in the pumps to provide for a simpler system design.

5. NUMERICAL SIMULATIONS

A. Simulation Model

Simulations are performed to understand the optical processes associated with the two-stage TDFA-based SC system. In the fiber, the complex envelope $A(z,t)$ of a pulse under the slowly varying approximation satisfies the GNLSE given by [27]

$$\frac{\partial A}{\partial z} = (\hat{D} + \hat{N})A, \tag{1}$$

$$\hat{D} = -\frac{i}{2}\beta_2\frac{\partial^2 A}{\partial \tau^2} + \frac{1}{6}\beta_3\frac{\partial^3 A}{\partial \tau^3} + \frac{i}{24}\beta_4\frac{\partial^4 A}{\partial \tau^4} - \frac{\alpha}{2},$$

with

$$\hat{N} = i\gamma\left(1 + \frac{i}{\omega_0}\frac{\partial}{\partial t}\right)\int_{-\infty}^{+\infty}[(1-f_R)\delta(t) + f_R h_R(t)]| \times A(z, t-t')|^2 \mathrm{d}t',$$

where the pulse moves along z in the retarded time frame $\tau = t - (z/\nu_g)$ with the central angular frequency of ω_0. The linear terms in the differential operator $\hat{D}$ account for the second (β_2), third (β_3), and fourth order (β_4) dispersion as well as the loss (α) of the fiber. The terms in the operator $\hat{N}$ result from nonlinear interactions, which describe self-phase modulation, self-steepening, and stimulated Raman scattering effects. In particular, the effective nonlinearity is defined as $\gamma = n_2\omega_0/cA_{\mathrm{eff}}$, where n_2 and A_{eff} are the nonlinear refractive index and effective mode area of the fiber, respectively. In

addition, $h_R(t)$ represents the Raman response function, and f_R is the fractional contribution of the Raman response to the nonlinear polarization.

The GNLSE described above is solved by a modified adaptive split-step Fourier method with the initial pulse shape as the known boundary value [16,28]. The step size is determined and dynamically adjusted by the nonlinear gain in each section. Super-Gaussian flat-top pulses with 80 ps FWHM with center wavelength at 1553 nm are used as input in the simulator. A temporal window of 100 ps and a spectral window of 333.33 THz are chosen to cover the entire SC spectrum, corresponding to 2^{16} sampling points. The Raman shift spectrum of fused silica and ZBLAN fibers as measured in [29] is used in the numerical analysis. The peak Raman gain coefficient (g_R) of fused silica fiber is set to 6.4×10^{-14} m/W at 1553 nm [16], and that of ZBLAN fiber is set to ~2.2 times that of fused silica [30]. The dispersion parameters of the standard SMF are approximated based on the fiber datasheet and that of the ZBLAN fiber from the measured material dispersion [24]. For standard SMF, an effective nonlinear parameter of $\gamma = 1.6\ \mathrm{W}^{-1}/\mathrm{km}^{-1}$ is used at 1553 nm [16]. Since the n_2 of ZBLAN is ~0.85 times that of fused silica [31], an effective nonlinear parameter of $1.36\ \mathrm{W}^{-1}\ \mathrm{km}^{-1}$ is used for the ZBLAN fiber. The loss (α) in the standard SMF (Corning) and ZBLAN fiber (KDD FiberLabs) used in the simulations is as per provided by the fiber manufacturers. To account for the dispersion of the mode profile in the ZBLAN fiber at longer wavelengths, the nonlinear gain is scaled inversely with wavelength based on a linear dependence of the mode field radius on wavelength. For example, the mode radius is expected to increase by ~1.65 times over 2 to 4 μm wavelength range based on numerical calculations, and the increase is approximated to be linear with wavelength. The bend-induced loss in the fiber is neglected due to the high NA and ~60 cm coiling diameter of the ZBLAN fiber in the experiments [1].

For modeling the TDFA, negative loss is assumed at wavelengths where gain is observed (1.95–2.13 μm). An experimentally measured TDFA gain profile is used in the simulations, with peak gain observed at 1980 nm. The dispersion of the gain fiber is assumed to be same as that of standard SMF, while the nonlinearity parameters are scaled in proportion to the core diameter of the gain fiber used in the experiments. In addition to the above components, the simulator also takes into account the effect of the pump combiner output fiber pigtail and the mechanical splice loss observed from the pump combiner output fiber to ZBLAN fiber, as observed experimentally.

B. Simulation Results

To verify the validity of the simulator, experimental results are compared to simulations. Figure 11 shows the comparison of the output spectrum from a 25 m length of standard SMF with 2.5 kW peak input power at 1553 nm as well as corresponding output from an 8.5 m length of ZBLAN fiber with ~12 dB of power gain in the TDFA stage, as observed in experiments. The figures show a single run of the simulation as well as an ensemble average of 12 simulation runs in comparison with the experimentally observed results. The single-run simulation output has several spectral features due to the smaller pulse width used in the simulation compared to experiments. Also, due to the averaging of the experimental spectral measurements with a lock-in time constant of 300 ms and 500 kHz system repetition rate, the measured spectrum shows an ensemble average over 150,000 instances of the 1.55 μm input pulse. The ensemble average of 12 simulation runs shows a trend toward reduction in the fluctuations in the spectrum as observed in the experimental results. The outputs of the different simulation runs show variation due to the evolution of the spectrum from background noise. The simulation output is also averaged over ~2 nm intervals to resemble the monochromator resolution in the experimental measurements.

Reasonable agreement in terms of spectral extent between experiments and simulations is observed for both the standard SMF and ZBLAN output cases. For the case of the fused silica SMF [Fig. 11(a)], the simulation output shows a longer extension of the output spectrum compared to experimental results, which is attributed to the larger mode profile dispersion in standard SMF due to an NA of ~0.13. For the case of ZBLAN output in Fig. 11(b), the simulations show higher depletion of the SC pump at ~2 μm compared to experimental results. This is attributed to the fact that the ZBLAN fiber has a cutoff wavelength of ~2.75 μm, which suggests some of the coupled 2 μm light in to the ZBLAN fiber may not be in the fundamental mode. These components would not contribute to the spectral broadening process due to lower field intensity of higher order modes and, hence, remain undepleted at the output of the ZBLAN fiber.

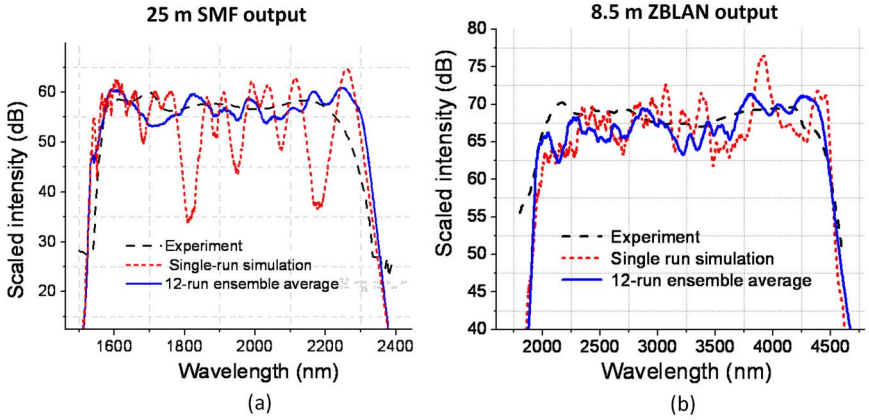

Fig. 11. (Color online) (a) Comparison of simulation versus experimental result at the output of 25 m standard SMF with 2.5 kW peak input power pulses at 1553 nm, (b) comparison of simulation versus experimental result for the output of 8.5 m ZBLAN at 12 dB power gain in the TDFA.

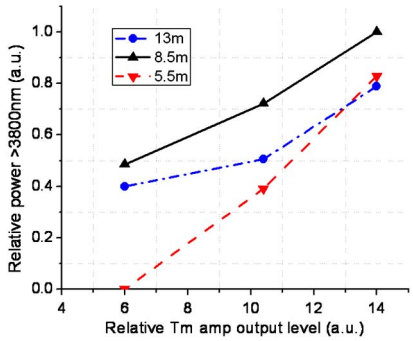

Fig. 12. (Color online) Simulation results for confirming dependence of efficiency in long wavelength generation on ZBLAN length.

In experiments, the efficiency of long wavelength generation is observed to be dependent on the ZBLAN fiber length for a given TDFA output power level. Simulations are performed to confirm the observed experimental results. For example, in Fig. 7, experimental results shows 8.5 m ZBLAN length to be more efficient in generation of wavelengths >3800 nm compared to 5.5 and 13 m ZBLAN lengths. Figure 12 shows the simulation results obtained for the relative power, i.e., area under the curve, beyond 3800 nm for 5.5, 8.5, and 13 m ZBLAN fiber lengths as a function of TDFA gain corresponding to ~3, ~5.2, and ~7 W of experimentally measured power-amp output. The observed results confirm a similar trend, where 8.5 m length shifts a larger fraction of the SC pump to wavelengths beyond 3800 nm.

Experimental results observed for the dependence on the 1.55 μm pulse peak powers on the 12 m ZBLAN output [Fig. 8(b)] contradict expectations. For a fixed amount of TDFA pump power, one would expect the input spectrum [Fig. 8(a)] corresponding to 2.5 kW peak power 1.55 μm pulses to give rise to the furthest extending spectrum. However, the observed results follow a trend that is opposite to this expectation. To verify the validity of the observed results, simulations are performed for two of the above measured cases. Figure 13 compares the experimental and simulation results for the 1.5 and 2.5 kW, 1.55 μm pulse peak power cases. Simulation results match the observed experiments, whereby lower 1.55 μm peak power pulses lead to longer extension of the ZBLAN output spectrum. The explanation of this phenomenon is observed in the time-domain evolution of pulses in the TDFA, shown in Fig. 13. It is observed that in the time domain, for the case of 2.5 kW, 1.55 μm peak power, more ~2 μm pulses evolve in the TDFA compared to the 1.5 kW case. As a result, the 2.5 kW, 1.55 μm pulse peak power case generates, at the output of the TDFA, a larger number of relatively low peak power ~2 μm pulses compared to the 1.5 kW case, which would explain the shorter extending spectrum out of the ZBLAN fiber compared to the 1.5 kW peak power case. Also, since the duty cycle in the 2.5 kW case is larger due to the presence of a larger number of 2 μm pulses, the ASE generation can be expected to be lower, leading to greater pump depletion.

In experiments, the long wavelength edge of the TDFA mid-IR SC spectrum extends longer than that from the EYFA-based system. Simulations are performed to compare the output from an 8.5 m length of ZBLAN fiber in the two systems. For the case of the EYFA system, input parameters used in

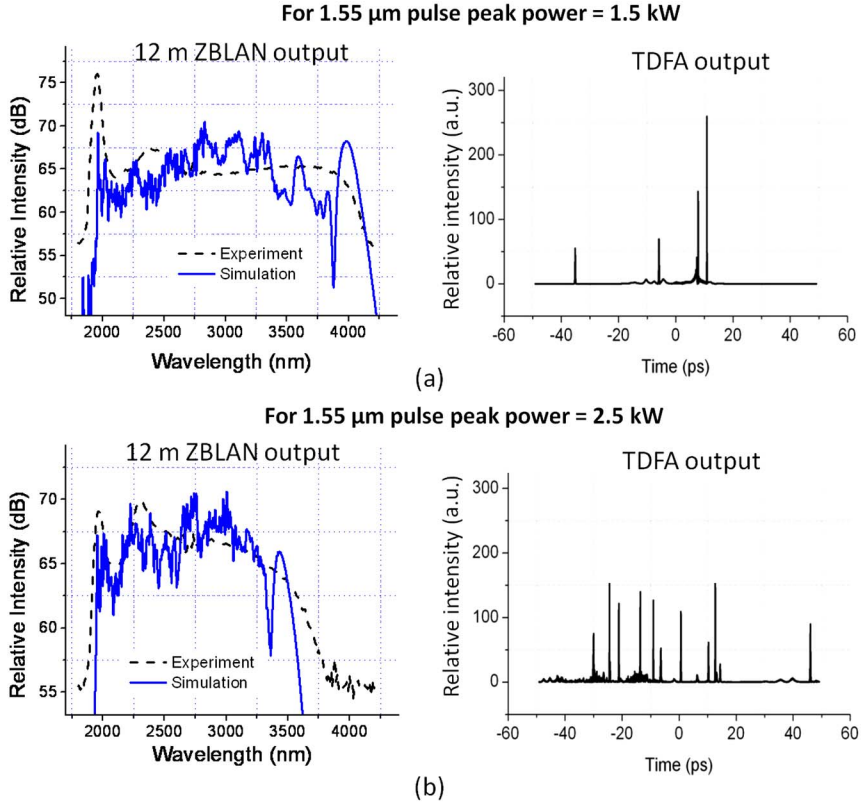

Fig. 13. (Color online) Simulation results for 1.55 μm peak power dependence on ZBLAN output: (a) spectral domain comparison between simulation and experiments for 1.5 kW and corresponding TDFA output time-domain pulse profile, (b) 2.5 kW peak power cases with ZBLAN spectral output comparison between experiments and simulations and corresponding TDFA output pulse profile.

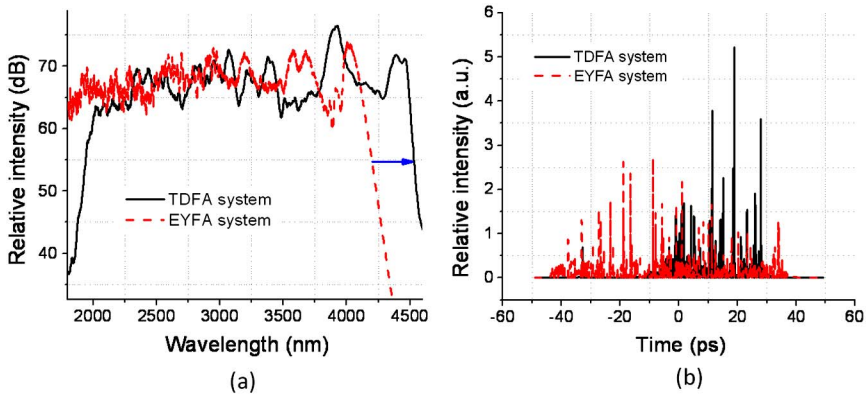

Fig. 14. (Color online) (a) Simulation results comparing output spectrum of 8.5 m length of ZBLAN fiber for EYFA and TDFA systems, (b) pulse profile comparison at the input of the ZBLAN fiber in the two power amp systems.

[17], specifically, 20 kW peak power pulse at 1.55 μm is input to an ~1 m length of standard SMF, and the output is propagated through an 8.5 m length of ZBLAN fiber after accounting for the mechanical splice loss. For the TDFA system, the single-run result shown in Fig. 11(b) is used. Figure 14(a) compares the output spectrum in the two cases, generating a spectrum at the output of the TDFA system extending ~330 nm further than the EYFA systems as observed in experiments. Figure 14(b) shows the corresponding input pulse profile to the ZBLAN fiber in the two systems. In the EYFA system case, simulations suggest that the MI-initiated pulse breakup process in the 1 m length of standard SMF after the Er:Yb amplifier stages gives rise to high peak power pulses responsible for long wavelength generation in the ZBLAN fiber. In the case of the TDFA system, simulations show that the amplification of wavelength-shifted components in a 25 m length of standard SMF around 2 μm yields a pulse profile with higher peak powers, which would explain the longer extending spectrum in the same length of ZBLAN fiber compared to the EYFA-based MISCL.

The long wavelength edge of the TDFA-based mid-IR SC is experimentally found to be limited to ~4.5 μm as shown in Fig. 5. Based on the fiber specifications, the loss in the ZBLAN fiber is expected to be ~1 dB/m at 4.5 μm, and the long wavelength edge seems to be loss-limited by the material absorption and poor confinement of longer wavelengths [1]. Simulations are performed to study the dependence of the loss profile of the ZBLAN fiber on the long wavelength edge. As shown in Fig. 15(a), three different loss profiles for the fiber displaced by around 200 nm from the manufacturer specifications are used in the simulator, and the corresponding output from 10 m length of ZBLAN fiber is shown in Fig. 15(b). It is observed that the long wavelength edge of the SC spectrum shifts in accordance with the loss curve, indicating that the SC long wavelength edge is limited by the loss in the ZBLAN fiber. For example, when the loss profile is shifted to lower wavelengths by ~200 nm, the long wavelength edge reduces by ~206 nm. Similarly, shifting the loss curve toward the longer wavelengths causes the SC output to shift by ~160 nm. The slightly lower shift in the SC edge compared to the shift in the loss is attributed to the mode profile dispersion, accounted for in the simulations.

6. DISCUSSION

We have demonstrated a TDFA-based mid-IR SC laser using a two-step nonlinear broadening setup. The observed advantages of such a system are manifold. First, it allows use of higher efficiency Tm-based systems compared to EYFAs. We have observed ~1.35 times higher pump-to-signal conversion efficiency in the LMA-TDFA compared to the Er:Yb power amplifier used in results demonstrated in [17]. Second, by shifting the SC pump to ~2 μm, a longer extending spectrum is obtained compared to the Er:Yb power-amp-based system. Specific to the case of ZBLAN fibers with ZDW ~1.65 μm, the TDFA system pumps the nonlinear medium in the anomalous dispersion regime and broadens spectrum more efficiently toward longer wavelengths through Raman processes. SC lasers pumped in the normal dispersion regime

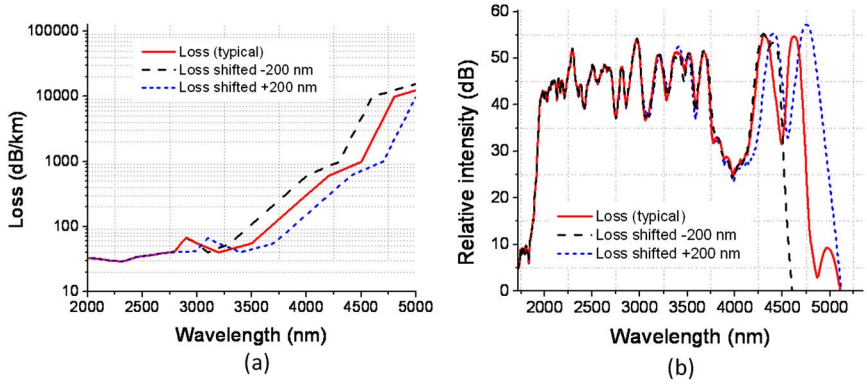

Fig. 15. (Color online) (a) Input loss profile for ZBLAN fiber into the simulator, (b) corresponding output spectrum from 10 m length of ZBLAN fiber.

[1,13,14,17], in comparison, broaden the spectrum toward either direction with respect to the pump wavelength. By further optimizing the experimental parameters, ~2.5 times higher optical efficiency in generating wavelengths beyond 3.8 μm is achieved in the thulium-based mid-IR SC laser compared to the previously demonstrated Er:Yb system [17].

The absolute efficiency of the LMA-TDFA seeded by a fused silica SC is currently observed to be ~27% with respect to 790 nm pump power. The observed efficiency is considerably lower than published numbers for Tm amplifiers. In particular, for the 25/250 μm LMA gain fiber used in our experiments, an absolute efficiency of ~53% has been demonstrated [18] in a CW lasing cavity configuration with respect to the launched pump power. In comparison, for our system, the signal loss in the splice at the gain fiber output end and the insertion loss of the output combiner currently amount to ~1 dB. In the absence of these losses, the expected TDFA efficiency is ~34.2%. Also, the generation of high peak powers leads to spectral broadening to ~2.5 μm in the ~0.5 m length of 10 μm core diameter fused silica fiber at the output of the pump combiner. Because of the phonon losses associated with the spectral shifting process, ~11% reduction is observed in the power-amp efficiency. The remainder of the gap in observed amplifier efficiency is attributed to the low duty cycle of the input signal to the amplifier. At a 500 kHz pulse repetition rate with a 1 ns long 1.55 μm pulse, the system duty cycle is set to 1:2000 with respect to the TDFA pump. However, at the output of a 25 m length of standard SMF, only a fraction of the 1.55 μm pulse shifts to the TDFA gain band, leading to a lower 2 μm signal duty cycle. The low input duty cycle results in larger losses to spontaneous emission in the amplifier and currently reduces the efficiency of the system.

An optical efficiency of ~9% is demonstrated for the TDFA-based mid-IR laser in converting 790 nm pump light to SC. In comparison, a QCL operating at room temperature generating 4.6 μm wavelength light with up to 8.8% wall-plug efficiency has been demonstrated [32]. Also, a $ZnGeP_2$-based OPO has been demonstrated with 22 W of output power in the 3–5 μm range and requiring 110 W of pump power, yielding a 20% optical conversion efficiency [9]. Another mid-IR OPO has been demonstrated based on a periodically poled MgO-doped congruent $LiNbO_3$ crystal capable of generating 16.7 W at 3.84 μm starting from 110 W at 1064 nm (15.2% optical conversion efficiency) [10]. Table 2 summarizes the results of these mid-IR light generation technologies in comparison to the demonstrated TDFA-based SC laser.

Our results show mid-IR SC generation with efficiencies approaching those of other technologies can be achieved with some improvements. One of the main loss components in the current system is the ~45% loss in the mechanical splice from the TDFA output to the ZBLAN fiber. Because of the dissimilar melting temperatures of fused silica and ZBLAN materials, fusion splicing of the two fibers is difficult. However, some preliminary work has been demonstrated in fused-silica-to-fluoride-fiber mechanical splices using a shape memory connector with losses as low as 0.8 dB at 1550 nm [33]. Incorporation of such a splice would increase the efficiency of the system by ~1.3 times. The splice loss from the LMA gain fiber to the combiner fiber is currently estimated to be ~0.6 dB, which can be reduced by better control and uniformity of the fusion temperature, which could not be achieved by our two-electrode arc-based splicer. The insertion loss of the combiner is observed to be ~0.4 dB and agrees with specifications provided by the manufacturer. Another approach to increasing the efficiency of the SC laser is by increasing the repetition rate of the 1.55 μm pulses. By increasing the duty cycle of the input pulses, higher amplifier efficiency can be achieved by reducing losses to spontaneous emission in the gain fiber. However, operation at higher repetition rates would also require more pump power and better thermal management to prevent damage to components due to the increase in the average power levels in the system.

Compared to the EYFA system, the Tm-based system generates a spectrum extending ~270 nm toward the longer wavelengths. Based on the simulation results shown in Fig. 14, we attribute the longer spectral edge to higher peak power pulses at the output of the TDFA compared to MI-initiated pulse breakup in a 1 m length of standard SMF following a Er:Yb power amplifier. The long wavelength edge of the SC spectrum obtained from the TDFA-based MISCL is limited to ~4.5 μm, as observed in Fig. 5. Because of pumping of the ZBLAN fiber in the anomalous dispersion regime, spectral broadening is dominantly Raman-induced soliton self-frequency shifting, as evidenced by the asymmetry of the spectrum around the 2 μm SC pump (Fig. 2). Based on the theoretical model proposed in [1] for MI-initiated Raman-based SC generation processes in step-index ZBLAN fibers, the edge of the SC is limited by the absorption loss in the fiber and the bend-induced loss. By using a fiber with a high NA of ~0.27 and coiling the fiber around a ~60 cm diameter cylinder, the effect of bend-induced loss is eliminated based on the calculations presented in [1], where negligible bend-induced loss is calculated for a ZBLAN fiber with comparable geometry. Using simulations we studied the effect of the absorption edge of the ZBLAN fiber on the SC edge. By shifting the loss edge, we observe a similar trend in the edge of the generated SC, showing that the long wavelength edge of the SC is largely dominated by the material loss in the fiber.

Table 2. Comparison of TDFA-Based Mid-IR SC Laser Efficiency with Other Mid-IR Lasers

Technology	Reference	Demonstrated Wavelength	Average Power Out	Demonstrated Efficiency	Advantages/Disadvantages
Quantum cascade laser	[32]	4.6 μm	1.5 W	8.8% (wall-plug)	High efficiency/single wavelength
ZGP-OPO pumped by hybrid Tm-fiber laser/Ho:YAG laser	[9]	3–5 μm tunable	22 W	20% (to 790 nm pump)	High average power, tunable/free-space optics
PPMgO-OPO pumped by *Q*-switched Nd:YAG laser	[10]	3.85 μm	16.7 W	15% (to Nd:YAG pump)	High average power/high beam M^2
TDFA-based mid-IR SC		2–4.5 μm	2.6 W	9% (to 790 nm pump)	Broad wavelength, no moving parts, remote fiber delivery/lower efficiency

One approach for longer wavelength generation using the TDFA-based high peak power source entails use of higher nonlinearity fibers. A tellurite PCF with ~10× the Raman gain coefficient compared to ZBLAN [30] and only 1.7 μm^2 mode field area has been demonstrated as a candidate for spectral generation up to ~4.8 μm with ~17 kW peak power 1.55 μm pulses coupled into an ~0.8 cm length of fiber with ~50% efficiency [14]. The results in Fig. 4 indicate that the TDFA-based 2 μm source should generate a spectrum extending beyond 4.5 μm in suitable tellurite PCFs, since we have shown a farther extending spectrum compared to the EYFA-system with ~20 kW peak power generation capabilities. However, to the best of our knowledge, maximum average power handling of only ~1.12 W in an 18 μm solid-core tellurite fiber has been demonstrated to date [34].

7. SUMMARY

We have demonstrated an all-fiber integrated, power scalable mid-IR SC laser based on a thulium-doped power amplifier stage. The laser generates a continuous spectrum extending from ~1.9 to 4.5 μm in an ~8.5 m length of high NA ZBLAN fiber with a core/cladding diameter of ~8/125 μm. Time-average power output of up to ~2.6 W with ~50% modulation is measured with ~0.7 W power in wavelengths beyond 3.8 μm.

An overall efficiency of ~9% is achieved in conversion of the 790 nm TDFA pump power to the SC output by optimizing the power-amp stage and the length of the ZBLAN fiber in the setup. Compared to previously demonstrated Er:Yb-based systems, ~2.5 times higher efficiency is observed in the conversion of power-amp pump to wavelengths >3.8 μm due to higher power-amp stage efficiency and shifting of SC pump to the mid-IR. An approximately 270 nm farther extending spectrum in the mid-IR is also obtained by generating higher peak power pulses at the output of the TDFA, as shown by the simulation results.

The novelty of our approach lies in the two-step SC generation. 2.5 kW peak power laser diode pulses at 1.55 μm are first shifted to beyond 2 μm in an ~25 m length of low near-IR loss standard SMF, based on a modulation instability-initiated SC generation process. The first stage SC is followed by a thulium-based LMA fiber amplifier, which provides gain for the ~2 μm wavelength components. Coupling the TDFA output to low mid-IR loss ZBLAN fiber gives rise to a second SC generating stage extending up to ~4.5 μm wavelength. Dependence of the parameters used in the generation of the first stage SC on the ZBLAN output was studied and optimized for increased long wavelength generation efficiency of the laser. Scaling of the SC average output power was also demonstrated, whereby similar spectral extent at increasing average powers is achieved by proportionately increasing the pulse repetition rate. Numerical simulations were also presented to verify the observed results, which indicate the long wavelength edge of the SC to be limited by the high absorption in the ZBLAN fiber beyond 4.5 μm.

The demonstrated fused silica SC-seeded TDFA system provides an alternative to mode-locked lasers at 2 μm for mid-IR light generation, while using all commercial off-the-shelf parts. The achieved optical efficiency in SC generation is currently limited by the high mechanical splice loss from the TDFA output fiber to the ZBLAN fiber and the low duty cycle of the input signal. With further optimization of these factors, mid-IR SC light generation with efficiency comparable to competing technologies such as OPOs can be achieved using TDFAs.

ACKNOWLEDGMENTS

This work was funded in part by the U.S. Army under project contract # W15P7T-10-C-H606 and the U.S. Air Force under project contract # FA9201-10-C-0110. The authors would like to thank B. Samson at Nufern for providing the gain fiber used in the experiments and C. Troutman at 3SAE Technologies and F. Martins at Nufern for input on splicing procedures for LMA fibers.

[†]Dr. Michael J. Freeman is the Director of Research at Omni Sciences Inc.

[§]Dr. Mohammed N. Islam is a Professor in the Electrical and Computer Engineering Department at the University of Michigan and is also the Founder, President, Chief Technology Officer and consultant to Omni Sciences Inc.

REFERENCES

1. C. Xia, Z. Xu, M. N. Islam, F. L. Terry Jr., M. J. Freeman, A. Zakel, and J. Mauricio, "10.5 W time-averaged power mid-IR supercontinuum generation extending beyond 4 μm with direct pulse pattern modulation," IEEE J. Sel. Top. Quantum Electron. **15**, 422–434 (2009).
2. S. T. Sanders, "A wavelength-agile source for broadband sensing," Appl. Phys. B **75**, 799–802 (2002).
3. H. Li, D. A. Harris, B. Xu, P. J. Wrzesinski, V. V. Lozovoy, and M. Dantus, "Standoff and arms-length detection of chemical with single-beam coherent anti-Stokes Raman scattering," Appl. Opt. **48**, B17–B22 (2009).
4. K.-D. F. Büchter, H. Herrmann, C. Langrock, M. M. Fejer, and W. Sohler, "All-optical Ti:PPLN wavelength conversion modules for free-space optical transmission links in the mid-infrared," Opt. Lett. **34**, 470–472 (2009).
5. C. R. Philbrick, D. M. Brown, A. H. Willitsford, P. S. Edwards, A. M. Wyant, Z. Z. Liu, C. T. Chadwick, and H. Hallen, "Remote sensing of chemical species in the atmosphere," presented at the Fourth Symposium on Lidar Atmospheric Applications, Phoenix, Arizona (January 11–15, 2009), http://ams.confex.com/ams/pdfpapers/150051.pdf.
6. I. T. Sorokina and K. L. Vodopyanov, eds., *Solid-State Mid-Infrared Laser Sources* (Springer-Verlag, 2003).
7. M. Razeghi, S. Slivken, Y. Bai, and S. R. Darvish, "The quantum cascade laser: a versatile and powerful tool," Opt. Photon. News **19**, 42–47 (2008).
8. Y. Bonetti and J. Faist, "Quantum cascade lasers: Entering the mid-infrared," Nat. Photon. **3**, 32–34 (2009).
9. E. Lippert, H. Fonnum, G. Arisholm, and K. Stenersen, "A 22 watt mid-infrared optical parametric oscillator with *V*-shaped 3-mirror ring resonator," Opt. Express **18**, 26475–26483 (2010).
10. Y. Peng, W. Wang, X. Wei, and D. Li, "High-efficiency mid-infrared optical parametric oscillator based on PPMgO:CLN," Opt. Lett. **34**, 2897–2899 (2009).
11. M. Pollnau and S. D. Jackson, "Advances in mid-infrared fiber lasers," in *Mid-Infrared Coherent Sources And Applications*, M. Ebrahim-Zadeh and I. T. Sorokina, eds. (Springer, 2008), pp. 315–346.
12. J. Mandon, E. Sorokin, I. T. Sorokina, G. Guelachvili, and N. Picqué, "Supercontinua for high-resolution absorption multiplex infrared spectroscopy," Opt. Lett. **33**, 285–287 (2008).
13. G. Qin, X. Yan, C. Kito, M. Liao, C. Chaudhari, T. Suzuki, and Y. Ohishi, "Ultrabroadband supercontinuum generation from ultraviolet to 6.28 μm in a fluoride fiber," Appl. Phys. Lett. **95**, 161103 (2009).
14. P. Domachuk, N. A. Wolchover, M. Cronin-Golomb, A. Wang, A. K. George, C. M. B. Cordeiro, J. C. Knight, and F. G. Omenetto, "Over 4000 nm bandwidth of mid-IR supercontinuum generation

in sub-centimeter segments of highly nonlinear tellurite PCFs," Opt. Express **16**, 7161–7168 (2008).
15. C. Xia, M. Kumar, M.-Y. Cheng, O. P. Kulkarni, M. N. Islam, A. Galvanauskas, F. L. Terry Jr., M. J. Freeman, D. A. Nolan, and W. A. Wood, "Supercontinuum generation in silica fibers by amplified nanosecond laser diode pulses," IEEE J. Sel. Top. Quantum Electron. **13**, 789–797 (2007).
16. C. Xia, M. Kumar, M.-Y. Cheng, R. S. Hegde, M. N. Islam, A. Galvanauskas, H. G. Winful, F. L. Terry Jr., M. J. Freeman, M. Poulain, and G. Mazé, "Power scalable mid-infrared supercontinuum generation in ZBLAN fluoride fibers with up to 1.3 watts time-averaged power," Opt. Express **15**, 865–871 (2007).
17. M. Kumar, Optical Sciences Laboratory, University of Michigan, 1301 Beal Avenue, Ann Arbor, Michigan 48109, USA, and M. N. Islam are preparing a manuscript to be called "Mid-infrared supercontinuum fiber laser-based stand-off reflection spectroscopy."
18. G. P. Frith and D. G. Lancaster, "Power scalable and efficient 790 nm pumped Tm^{3+}-doped fiber lasers," Proc. SPIE **6102**, 610208 (2006).
19. A. Carter, J. Farroni, K. Tankala, B. Samson, D. Machewirth, N. Jacobson, W. Torruellas, Y. Chen, M. Cheng, A. Galvanauskas, and A. Sanchez, "Robustly single-mode polarization maintaining Er/Yb co-doped LMA fiber for high power applications," in *Conference on Lasers and Electro-Optics/Quantum Electronics and Laser Science Conference and Photonic Applications Systems Technologies* (Optical Society of America, 2007), paper CTuS6.
20. G. Imeshev and M. Fermann, "230 kW peak power femtosecond pulses from a high power tunable source based on amplification in Tm-doped fiber," Opt. Express **13**, 7424–7431 (2005).
21. K. Kieu and F. W. Wise, "Soliton thulium-doped fiber laser with carbon nanotube saturable absorber," IEEE Photon. Technol. Lett. **21**, 128–130 (2009).
22. P. T. Rakich, Y. Fink, and M. Soljačić, "Efficient mid-IR spectral generation via spontaneous fifth-order cascaded-Raman amplification in silica fibers," Opt. Lett. **33**, 1690–1692 (2008).
23. M. Jiang and P. Tayebati, "Stable 10 ns, kilowatt peak-power pulse generation from a gain-switched Tm-doped fiber laser," Opt. Lett. **32**, 1797–1799 (2007).
24. J. A. Harrington, *Infrared Fibers and Their Applications* (SPIE, 2004).
25. D. L. Auble and T. P. Meyers, "An open path, fast response infrared absorption gas analyzer for H_2O and CO_2," Bound.-Lay. Meteorol. **59**, 243–256 (1992).
26. S. D. Agger and J. H. Povlsen, "Emission and absorption cross section of thulium doped silica fibers," Opt. Express **14**, 50–57 (2006).
27. G. P. Agrawal, *Nonlinear Fiber Optics* (Academic, 2001).
28. G. Chang, T. B. Norris, and H. G. Winful, "Optimization of supercontinuum generation in photonic crystal fibers for pulse compression," Opt. Lett. **28**, 546–548 (2003).
29. A. Saissy, J. Botineau, L. Macon, and G. Maze, "Raman scattering in a fluorozirconate glass optical fiber," J. Phys. Lett. **46**, 289–294 (1985).
30. M. D. O'Donnell, K. Richardson, R. Stolen, C. Rivero, T. Cardinal, M. Couzi, D. Furniss, and A. B. Seddon, "Raman gain of selected tellurite glasses for IR fibre lasers calculated from spontaneous scattering spectra," Opt. Mater. **30**, 946–951 (2008).
31. X. Zhu and N. Peyghambarian, "High-power ZBLAN glass fiber lasers: review and prospect," Adv. Optoelectron. **2010**, 501956 (2010).
32. A. Lyakh, C. Pflügl, L. Diehl, Q. J. Wang, F. Capasso, X. J. Wang, J. Y. Fan, T. Tanbun-Ek, R. Maulini, A. Tsekoun, R. Go, C. Kumar, and N. Patel, "1.6 W high wall plug efficiency, continuous-wave room temperature quantum cascade laser emitting at 4.6 μm," Appl. Phys. Lett. **92**, 111110 (2008).
33. D. Faucher, A. Fraser, P. Zivojinovic, X. P. Godmaire, É. Weynant, M. Bernier, and R. Vallée, "High power handling shape memory alloy optical fiber connector," Appl. Opt. **48**, 5664–5667 (2009).
34. K. Li, G. Zhang, and L. Hu, "Watt-level ~2 μm laser output in Tm^{3+}-doped tungsten tellurite glass double-cladding fiber," Opt. Lett. **35**, 4136–4138 (2010).